

Active Control of Far-Field Noise from a Ducted Propeller

Daniel L. Sutliff* and Robert T. Nagel†

North Carolina State University, Raleigh, North Carolina 27695

A feedforward control algorithm using a rpm reference signal and a rotor position signal was used to apply active noise control to reduce the far-field noise generated by a ducted propeller. This technique reduced the noise radiated from the plane wave and first circumferential (1, 0) spinning duct mode. Simultaneous cancellation of the blade passing frequency and the first harmonic was achieved. These reductions were obtained over a wide range of far-field angles with no increase in noise at other frequencies.

Introduction

ACTIVE noise control (ANC) offers potential for effective elimination of far-field tones radiating from ducted rotor systems. Three main classes of algorithms for ANC are possible: power sensing, where the acoustic power is detected and minimized; transform methods for which the controlling parameters in the form of coefficients are sought so as to minimize the noise; and finally, waveform synthesis for which considerable information about the acoustic pressure field must be known. Each method is capable of yielding 20 dB or more of noise reduction but the methods vary significantly in the time and complexity required for adjustment to variations in the subject noise. Waveform synthesis techniques typically require less than 1/10 of the adaptation time required of the other two methods.

A type of waveform synthesis technique using a rpm monitor was used by Koopman et al.¹ and Neise and Koopman² to control centrifugal fan noise within the duct. This work achieved creditable results. Quinlan³ canceled noise from an axial flow electrical equipment cooling fan with the antisource in the plane of rotation and reported only the resulting noise at the error microphone location; 10 dB of acoustic power reduction was reported. Eriksson et al.⁴ reduced the plane wave and the (1, 0) mode from two speakers in a rectangular duct. Reductions of the plane wave were greater than those of the (1, 0) mode.

The most famous application of ANC may be the reduction of noise achieved by Ffowcs-Williams⁵ on the British Gas Corporation gas turbine test stand. Few details of the arrangement are provided but the system is extremely successful in a deleterious environment. Active control of turbofan engine inlet noise was also attempted by Burdisso et al.⁶, again using an adaptive feedforward control. This transform method was able to reduce noise at the error microphone location, but far-field noise increased at many other sideline positions.

Successful application of ANC to ducted rotors using waveform synthesis requires an understanding of the acoustic characteristics of a rotating pressure source in a duct as described by Tyler and Sofrin⁷ and Rice et al.⁸ The generation of circumferential modes by a rotor-stator configuration is well known with mode numbers given by

$$m = sB + kV \quad (1)$$

where B and V are the number of blades and vanes respectively, s is the harmonic number, and k is an integer index. The pressure patterns and rotational speeds of these modes may be considered

deterministic. The frequency and phase of the antisource necessary to cancel the modes are related to the rpm and circumferential position of the rotating blades respectively. The pressure amplitudes depend on the blade loading.

The method employed in this experimental study uses waveform synthesis utilizing both rpm and blade position. Data for the time history of one period of a nondimensional sine wave is generated at startup with a PS/2 personal computer. This base sine wave is shifted to the measured frequency and phase, as determined from the measured blade position, required to cancel the subject noise near the antisource location. The scaling of the basic waveform is done in real time and sent to speakers within the rotor duct.

Experimental Setup

A 0.305-m- (1-ft-) diam, 2.13-m- (7-ft-) long circular duct with a nearly bellmouth inlet houses a 27.94-cm- (11-in.-) diam hobby craft model propeller. The propeller is driven by an ac motor, belt and pulley system. The antinoise sources are four 7.62-cm- (3-in.-) diam, 100-W speakers, each mounted in an adjustable baffle. The speakers are circumferentially distributed in the wall of the duct in a plane near the bellmouth inlet. The test rig, as shown in Fig. 1, is installed in the North Carolina State University Center for Sound and Vibration anechoic chamber. The chamber is anechoic to 125 Hz, well below the minimum blade passing frequency (BPF) of 350 Hz. The test article is positioned off the centerline of the chamber to eliminate the possibility of standing waves, and the arc of far-field noise measurement is at least a 1/4 wavelength away from the chamber walls.

The test rig was operated with two- or four-bladed propellers. The four-bladed propeller was used with or without fixed vanes. The vanes, when installed, were placed approximately 1/2 the chord length upstream of the blades. The vanes were simple flat plate sections with variable angle of attack. Three vanes were used with four propeller blades to produce a (1, 0) duct mode. Higher modes were cut off as discussed later.

The frequency and phase information required to scale the base sine wave is measured directly from the rotor shaft using two separate light emitting diode (LED) systems. The rpm is accurately determined from a 45 pulse per revolution signal. The ordinary coherence between this LED generated rpm signal and the far-field acoustic signal at BPF was typically $\gamma^2 = 0.99$. The blade position during the rotation is determined from a once per revolution signal obtained at top dead center of the circumferential track. These data are input to the computer with an analog-to-digital (A/D) system and used to periodically update the antisource signal. The LED information is regularly updated in the computer and the antisource signal is continually output to the speakers.

Control Algorithm

A rpm feedforward control algorithm is used to determine the antinoise output. The algorithm determines the output frequency from the rpm signal as discussed earlier. Since the computational speed of the PS/2 model 70 is insufficient for real time processing, a scaling

Received Aug. 23, 1993; presented as Paper 93-4356 at the AIAA 15th Aeroacoustics Conference, Long Beach, CA, Oct. 25-27, 1993; revision received April 12, 1994; accepted for publication April 13, 1994. Copyright © 1994 by the American Institute of Aeronautics and Astronautics, Inc. All rights reserved.

*Research Assistant, Aerospace Engineering, Center for Sound and Vibration. Member AIAA.

†Professor of Aerospace Engineering and Director, Center for Sound and Vibration. Member AIAA.

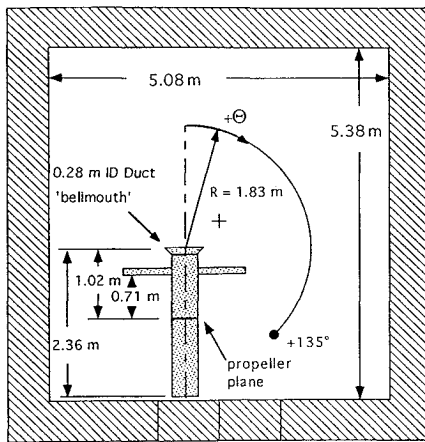


Fig. 1 Duct/rotor system and acoustic measurement locations within anechoic chamber.

algorithm was employed. Essentially, the nondimensional amplitudes of the high-resolution sine wave (30,000 points) are stored in a permanent array. The desired output is determined by scaling the nondimensional array based on the frequency and the known modal structure of the acoustic wave propagating in the duct. A slight loss in frequency resolution occurs in this process.

Frequency, phase, and amplitude information required to synthesize the antisource signal are available within the control program. An error microphone is not required during operation of the ANC system. The acoustic and instrumentation based phase shifts are determined off line as a function of frequency. Determination of the characteristics of the original noise and antisources prior to operation may be called off-line system identification. The primary acoustic phase shifts are due to propagation of the fan noise in the duct, the speaker baffle tube which modifies the phase of the input antinnoise, and the final 180 deg phase shift required for cancellation. There are several additional minor phase changes imposed by instrumentation, etc. All of these phase changes are converted to time delays which are functions of the blade rotation frequency. The total sum time delay is applied to the antisource signal and synchronized with the propeller noise using the blade position LED signal. The blade position provides the required phase information for the actual propeller noise. The propagation of this noise along the duct is understood from well-established theory.^{7,8}

When canceling the (1, 0) spinning mode, an additional phase shift, or time delay, is imposed on each speaker in sequential order progressing circumferentially around the duct. This means a phase shift of 0, 90, 180, and 270 deg is added to speakers 1–4 respectively, in the proper rotational direction so as to ensure the correct rotation of the antisource spinning mode.

The amplitudes of the source and antisource signals, as determined by measurements at a single far-field location, are functions of rpm. This amplitude information is also acquired prior to operation. A provision exists in the code for amplitude variations with frequency, but as the motor used in this experiment did not have rpm variation capabilities this could not be demonstrated. The frequency dependent phase and amplitude relationships do not change unless the test rig is reconfigured, i.e., a change of blades or duct. The system identification thus need not be repeated each time the ANC algorithm is used.

There is a small amount of parallel processing through the A/D and a small but periodic down time due to the relatively slow PS/2 model 70 computer used.

Data Collection

Effectiveness of this noise reduction system is evaluated at the frequency of concern by comparing the far-field sound pressure level (SPL) with and without the ANC system. A 1/2-in. free-field microphone and a two-channel fast fourier transform (FFT) spectrum analyzer were used for the data analysis. The waterfall slice mode of the analyzer is suitable for this data analysis. The resulting series of power spectrum density (PSD) plots are displayed and a

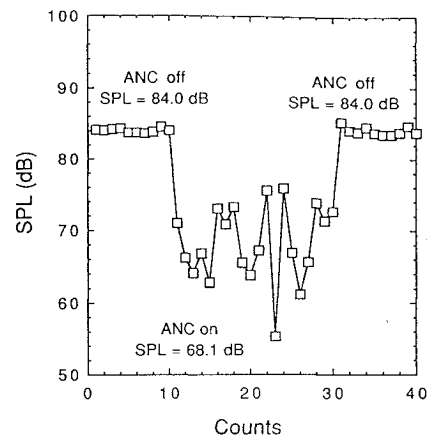


Fig. 2 Typical time history of far-field SPL showing ANC with two antisource speakers.

frequency slice is selected to provide a time history of the SPL vs counts at the selected frequency. This frequency is the fan BPF or its harmonics. An example of such a time history is shown in Fig. 2. Each count represents the average of approximately 1.2 s of data with the 40-count series representing approximately 60 s of data.

To compare results with and without ANC, a switch is installed which simply disconnects the antisource speaker system. Figure 2 shows data with 10 counts obtained with the ANC system switched off, followed by 20 counts with the system on, and then a final 10 counts with the system again switched off. The average of those 20 counts with the ANC system off minus the average with the system on defines the average level of reduction achieved (Δ SPL). The entire slice is saved as one data point providing the resulting level of noise reduction.

The data were taken in the far field at polar angles over the range $-135 < \Theta < +135$ deg and at radii from the duct inlet plane $0 < R < 2.44$ m.

Results

This control system was applied to the plane wave (0, 0) mode, and the first-order circumferential mode (1, 0). The effects of varying the number of antisources were investigated along with the simultaneous control of the blade passing frequency and the first harmonic at $2 \times$ BPF.

Control of the Plane Wave

The reduction of the plane wave was examined with respect to antisource frequency, amplitude, and phase. These results, more fully discussed in Ref. 9, show the loss of attenuation as the antisource is moved from the optimum setting. In addition, the relative effectiveness of using one, two, or four active antisource speakers was examined for the plane-wave case generated by a two-bladed propeller and two fixed vanes. Figure 3 shows the SPL reduction in decibels at the far-field location on the duct centerline as a function of imposed phase error Φ .

When two speakers are used they are diametrically opposed. One speaker at the proper phase shift of 180 deg provides about 14 dB of noise reduction. Two antisources produce about 5–6 dB additional reduction. The lack of further noise reduction with four antisources occurs because the tone is reduced (in the narrowband spectrum) to the broadband floor by the two-speaker case, and no additional reduction is possible.

As the phase of the antisource is varied from 180 deg, the two- and four-speaker cases do not degrade as quickly as the single-speaker case. This may be attributable to improved circumferential symmetry associated with the two- and four-speaker cases.

A special concern when considering aircraft noise is directivity. The directivity of the uncontrolled propeller SPL, the speaker SPL, and the reduced SPL is in Fig. 4. The far-field amplitudes of the uncontrolled propeller and the speaker output match well, especially

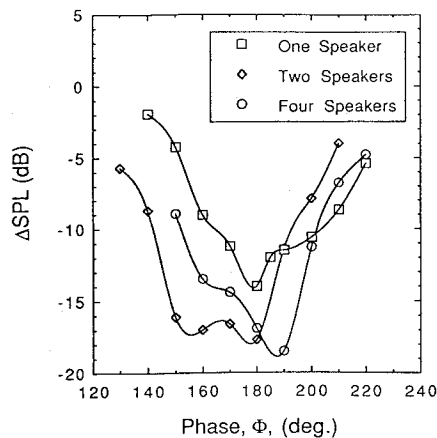


Fig. 3 Far-field noise reduction as a function of antisource phase for various active antisources; (0, 0) mode.

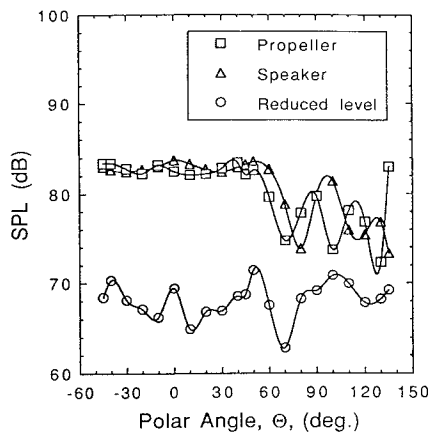


Fig. 4 SPL directivity of propeller and speakers, and the reduced level with two antisource speakers.

at polar angles Θ less than 60 deg. Reduction in the controlled level occurs over the entire range of far-field angles surveyed.

The reduction obtained with one, two, or four active antinoise sources is compared in Fig. 5. A variation in the directivity occurs for $\Theta > 60$ deg. An apparent loss in the noise reduction occurs at $\Theta = 80$ deg with one antisource speaker active and at 100 deg with two speakers active. This can be accounted for by noting that a local minimum in the uncanceled SPL occurs at these angles as shown in Fig. 4. Attenuation below the broadband level is not expected. This loss is not apparent when four speakers are active, but the number of data points are fewer. Four antisource speakers do not increase the maximum attenuation but may extend the beneficial effects over a wider far-field angle range as shown between 30 and 80 deg in Fig. 5.

When applying ANC to real sources it is likely that the theoretical maximum reduction cannot be achieved due to errors in source/antisource superposition. Errors may occur in amplitude, frequency, or phase as listed in Table 1. To estimate the effect of errors, a sensitivity factor is computed by linearizing the slope near the maximum reduction. Examples of errors in phase are seen in Fig. 3. Phase sensitivity is ≈ 3.2 -dB loss in reduction per 10-deg phase error.

The antisource frequency was also deliberately set to an erroneous value with expected losses in noise reduction occurring. Frequency errors can also occur as a result of fluctuations in the rpm. The average change in BPF over 1 s is monitored and recorded. These types of frequency errors arise from different mechanisms, yet have similar influences. The noise reduction sensitivity to both types of frequency errors is ≈ 4.0 dB/0.1 Hz.

In addition to a phase error in the overall ANC system, a phase mismatch between two speakers within the system can occur. The effects of this possibility were tested by driving one speaker at the

Table 1 Summary of parametric effects

Error in	Sensitivity parameter		
	Dimensional	Nondim.	3-dB loss
Phase	3.2 dB/10 deg	18 dB/rad	10 deg
Amplitude	3.5 dB/dB	3.5 dB/dB	1 dB
Frequency	4.0 dB/0.1 Hz	6.4 dB/(rad/s)	0.1 Hz
Phase mismatch	2.1 dB/10 deg	12 dB/rad	15 deg

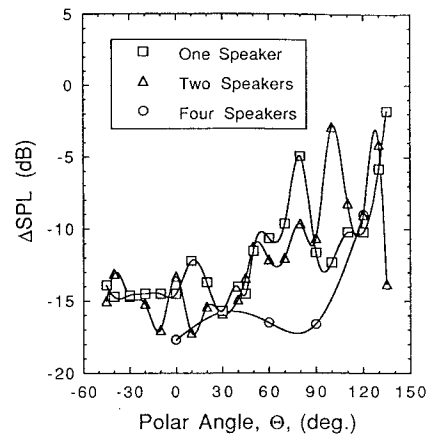


Fig. 5 Directivity of reduction achieved from one, two, or four anti-source speakers.

proper phase, and the second speaker was operated at a nonoptimum phase. The sensitivity of noise reduction to a phase error for this case is ≈ 2.1 dB/10 deg; less than the case when both speakers are in error.

Driving the speakers at a different phase relative to each other naturally causes a drop in the far-field amplitude due to superposition. This was compensated for and is not the reason for the reduction loss.

Nondimensionalizing the sensitivity parameters yields a comparison of their relative importance. Nondimensional frequency sensitivity is 6.4 dB-s/rad. Converting degrees to radians, the phase sensitivity is 18 dB/rad. Therefore, for an output time scale of 1 s, the noise reduction is approximately three times as sensitive to phase errors when compared to frequency errors. Table 1 summarizes these results.

Simultaneous Control of the Fundamental and First Harmonic

The fundamental tone (BPF) and first harmonic ($2 \times$ BPF) were independently canceled in separate experiments. Simultaneous cancellation of these tones was also investigated. For the two-bladed propeller both the frequency of the fundamental tone at BPF and the first harmonic at $2 \times$ BPF are below the cutoff frequencies and therefore excite only the plane wave. For the simultaneous cancellation, one pair of opposed speakers is used to cancel the fundamental, whereas the second pair of opposed speakers cancels the first harmonic. Figure 6 compares the uncanceled PSD to the PSD with simultaneous cancellation applied. These data were taken at $R = 1.83$ m (6 ft), $\Theta = 30$ deg. A reduction of about 19 and 17 dB is achieved at the BPF and $2 \times$ BPF respectively.

The directivity of the simultaneous cancellation is shown in Fig. 7. Figure 7a compares the reduction in the fundamental tone for two cases; the reduction at the BPF when cancellation is applied solely to that tone, and the reduction achieved at the BPF when cancellation was applied simultaneously to the BPF and $2 \times$ BPF. Figure 7b makes a similar comparison, except the reduction in the first harmonic is shown. The reduction levels of the first harmonic exhibit some variability but this is because the phase and frequency of the harmonic are based on a multiple of the fundamental phase and frequency. This causes a higher uncertainty in the output at the first harmonic and magnifies any existing fluctuations, slightly reducing the coherence with the rpm signal.

The two figures show no significant interference caused by simultaneous cancellation. No significant change in the SPL amplitude at

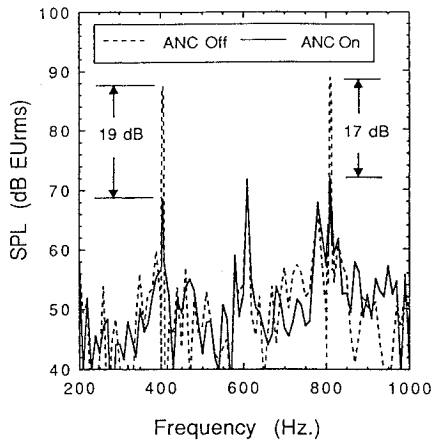
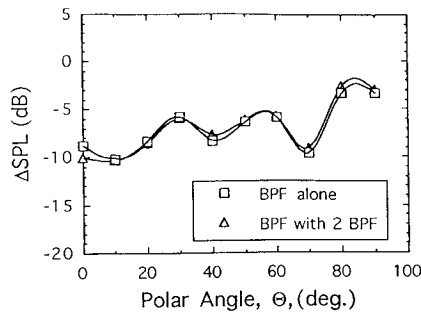
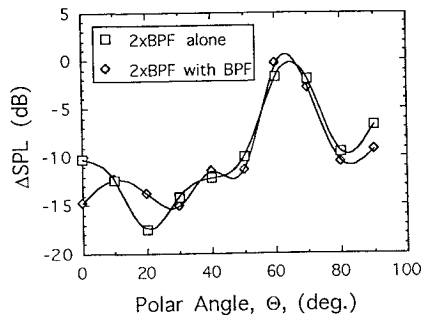


Fig. 6 PSD showing simultaneous reduction of BPF and $2 \times$ BPF with two antisource speakers for each tone.



a) Reduction in fundamental at 405 Hz



b) Reduction in 1st harmonic at 810 Hz

Fig. 7 Directivity of reduction at BPF and $2 \times$ BPF individually and simultaneously with two active antisource speakers for each tone.

other frequencies occurs, including those higher than 1 kHz. This is obviously a case of superposition, valid because the noise levels are well within the linear acoustic range.

Control of the (1, 0) Mode

Cancellation of the plane wave is relatively straightforward due to its one-dimensional nature. The cancellation of higher order modes is more difficult as their propagation is not one dimensional. The antisource speakers must respond in circumferential order with phase locked to the spiralling pressure pattern of the mode.

The test rig was modified to run a four-bladed propeller with three flat upstream vanes mounted on the duct wall to generate the (1, 0) spinning mode. This added resistance required a higher powered motor which turned the shaft at approximately 202 Hz yielding a BPF of 810 Hz. From Eq. (1), $m = sB + kV = (1)(4) + k(3)$, where m is the circumferential mode number, s the harmonic number, B the number of blades, k an integer ranging over all values, and V the number of stator vanes.

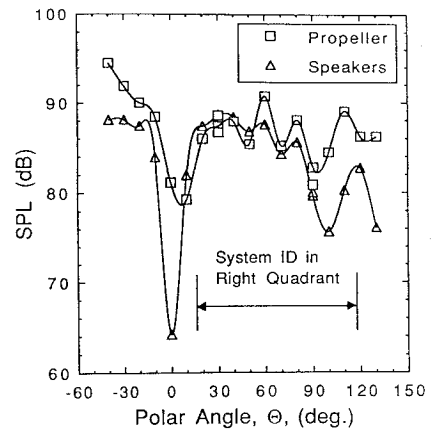


Fig. 8 Directivity of speakers and propeller for right quadrant system identification; (1, 0) mode with two antisource speakers.

Each m -lobe pattern rotates at a different speed given by

$$\Omega_m = \frac{\Omega}{(1 + kV/sB)} = \frac{\Omega}{(1 + 3k/4s)} \quad (2)$$

where Ω and Ω_m are the shaft and mode rotational velocities, respectively. Since the tip speed is subsonic, only values of k leading to $\Omega_m > \Omega$ could possibly propagate. The fundamental tone ($s = 1$) requires $-3 < k < 0$ for possible propagation. The only mode propagating at the fundamental frequency is the $m = 1$ mode, and it rotates four times the shaft speed in the same direction as the blade rotation.

Below the cutoff frequency the pressure disturbance is not truly wave propagation and decays exponentially along the duct axis. The ratio of the axial wavenumber to the duct diameter is so small that the full cycle phase variation, which is the defining characteristic of a higher mode, cannot exist.

An infinite number of radial modes can also exist for each circumferential mode. If the circumferential mode decays, so do the radial modes associated with that circumferential mode. Only if a circumferential mode propagates can the associated radial modes possibly propagate. The cutoff frequency (from the hardwall eigenvalues) for the (1, 1) mode is 1340 Hz for this apparatus. The radial modes do not propagate for this experimental setup.

The existence of the (1, 0) mode was verified using the two-microphone method. Two microphones placed on the inner duct wall verified that the phase of the pressure varied directly with relative circumferential position of the microphones. For example, the pressure signal of microphones geometrically separated 180 deg are in phase for the plane wave, but 180 deg out of phase for the (1, 0) mode. Data from several relative microphone positions verified that the dominant pressure pattern in the duct was caused by the (1, 0) mode as expected.

Figure 8 shows the far-field SPL vs polar angle for the speakers alone and the uncanceled propeller noise. The speakers produce a dramatic minimum at $\Theta = 0$ deg, indicating a very clean (1, 0) mode. The SPL amplitude of the uncanceled propeller noise shows a minimum not at $\Theta = 0$ deg, but at 10 deg, and not nearly as dramatic. Furthermore there is an asymmetry, with the levels in the left quadrant being several decibels higher than those in the right quadrant (compare -45 deg and $+45$ deg). The (1, 0) mode is the dominant mode, but it is not pure. This may be due to inlet/duct/propeller misalignment. These anomalies are attributed to this particular apparatus and are considered to be unimportant. To obtain the far-field SPL asymmetry with two antisources located in the same duct plane was impossible as their superposition in the duct yields a uniform radiation of the (1, 0) mode.

Because of this asymmetry, cancellation was attempted by quadrant. Unlike the plane-wave case, where the reduction obtained was independent of the location where the amplitude was measured, the attenuation of the (1, 0) mode was quadrant dependent. The noise level for the left and right quadrants should be the same, but with this apparatus there is a difference. One side or the other must be

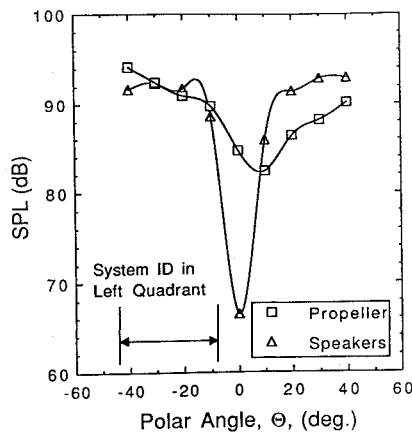


Fig. 9 Directivity of speakers and propeller for left quadrant identification; (1, 0) mode with two antisource speakers.

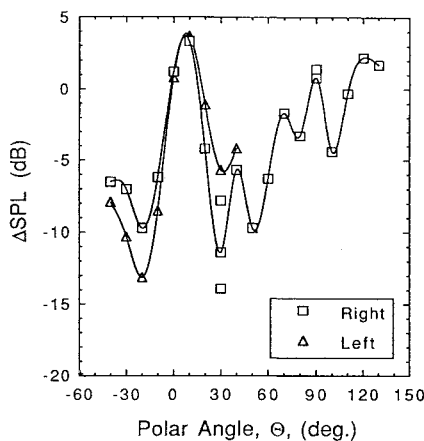


Fig. 10 Directivity of the reduction achieved with left and right system identification; (1, 0) mode with two antisource speakers.

selected as an input on which to base the amplitude of the antisource output levels. Since the SPL at $\Theta = 0$ deg is nonexistent in theory, we cannot choose the centerline level. The maximum SPL occurs at $\Theta = \pm 30$ deg, so this angle was chosen as the location to obtain the system identification of the amplitude, depending on which quadrant the cancellation was emphasized. Thus, in Fig. 8 the system identification was done in the right quadrant.

Figure 9 shows the directivity of the uncontrolled propeller noise level and the speaker noise with the system amplitude identification emphasized in the left quadrant. The SPL of the uncontrolled propeller and the speaker agree best near $\Theta = -30$ deg.

The reduction obtained for these two cases is shown in Fig. 10. Noise reduction occurs over most of the range of far-field angles except near $\Theta = 0$ deg. The increase at these angles is small, and it is more than compensated for by the larger reductions over the majority of polar angles. The net overall SPL is reduced. Substantial cancellation occurs in both the left and right quadrants regardless of the quadrant in which the system identification was performed. The cancellation for a particular quadrant is, however, about 4 dB better if the system identification was performed there. This indicates that the mode is being canceled in the duct as a whole and then radiates in a weakened condition, rather than being canceled locally outside the duct.

The results from cancellation of the (1, 0) mode with four antisource speakers is shown in Fig. 11. Four active speakers yield reduction of the SPL throughout the entire range of polar angles. The better performance, especially at $\Theta = 0$ deg, is due to the more uniform circumferential distribution with four speakers.

When generating an antisource (1, 0) spinning mode with only two active antisource speakers, the speakers are activated 180 deg out of phase to generate the required acoustic pressure pattern. Unlike the case with four active speakers, the direction of rotation is not established by the incremental 90-deg phasing of each successive

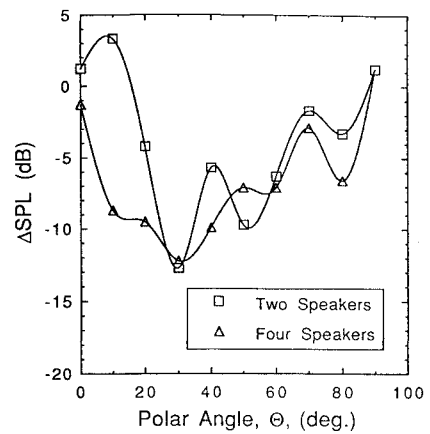


Fig. 11 Directivity of reduction achieved with two and four antisource speakers.

speaker. The rotational sense of a mode generated by two identical and perfectly opposed and phased speakers can not be determined. Such an ideal case would generate a nonrotating pressure pattern propagating axially but standing in the circumferential direction θ . In actuality, speakers are not perfectly positioned in the duct wall and do not direct their output precisely to the center of the duct. This may be caused by alignment errors or asymmetries in the mechanical response of the speaker diaphragm. A spinning (1, 0) mode from only two speakers has a preferred direction which depends on the speaker installation. The quality of the mode can be enhanced with proper selection of the input phase. Details of this phenomenon are presented in Ref. 10.

Conclusions

Measurements show that digital feedforward active control using input from a blade position sensor is a simple and very effective approach to attenuate tones from a ducted propeller system. No on-line error microphone is required with this method. The BPF and its harmonics can be simultaneously controlled as well as spinning modes. This work has shown effective control of the (1, 0) mode and the plane wave (0, 0) mode. Noise reduction is realized with this technique over a wide range of far-field angles without an increase in the SPL at other angular locations. It is also note worthy that the SPL does not increase at other frequencies. The update time with this technique is small compared to other methods, and the results are effective in yielding reductions near the noise floor as defined by the broadband level.

The method used in this study utilizes available knowledge about fan noise propagation in ducts, including well-documented information on spinning modes. Use of this known information permits an effective ANC system with a very simple computational scheme that may be run on an extremely modest computer. In addition, the system identification need not be repeated at each start up.

Acknowledgment

The authors wish to acknowledge the NASA Lewis Research Center for partial support of this work under Grant NAG 3-855.

References

- Koopman, G. H., Neise, W., and Chen, W., "Active Noise Control to Reduce the Blade Tone Noise of Centrifugal Fans," *Journal of Vibration, Acoustics, Stress, and Reliability in Design*, Vol. 110, July 1988, pp. 377-383.
- Neise, W., and Koopman, G. H., "Active Source Cancellation of the Blade Tone Fundamental and Harmonics in Centrifugal Fans," *Inter-Noise 88: The Sources of Noise*, Proceedings of the 1988 International Conference on Noise Control Engineering, Noise Control Foundation, Poughkeepsie, NY, 1988, pp. 801-804.
- Quinlan, D., "Active Control of Noise Radiated from Small Axial Flow Fans," *Inter-Noise 89: Engineering for Environmental Noise Control*, Proceedings of the 1989 International Conference on Noise Control Engineering, Noise Control Foundation, Poughkeepsie, NY, 1989, pp. 479-482.
- Eriksson, L. J., Allie, M. C., Hoops, R. H., and Warner, J. V., "Higher

Order Mode Cancellation in Ducts Using Active Noise Control," *Inter-Noise 89: Engineering for Environmental Noise Control*, Proceedings of the 1989 International Conference of Noise Control Engineering, Noise Control Foundation, Poughkeepsie, NY, 1989, pp. 495-500.

⁵Ffowcs-Williams, J. E., "The Silent Noise of a Gas Turbine," *British Science News*, Vol. 175, No. 1, 1981, pp. 9-12.

⁶Burdisso, R. A., Thomas, R. H., Fuller, C. R., and O'Brien, W. F., "Active Control of Radiated Inlet Noise from Turbofan Engines," *Proceedings of the Second Conference on Recent Advances in Active Control of Sound and Vibration*, Technomic Publishing Company, Inc., Lancaster, PA, 1993, pp. 848-960.

⁷Tyler, J. M., and Sofrin, T. G., "Axial Flow Compressor Noise Studies," *SAE Transactions*, Society of Automotive Engineers, Technomic Publishing

Company, Inc., Lancaster, PA, Vol. 70, 1962, pp. 309-332.

⁸Rice, E. J., Heidmann, M. F., and Sofrin, T. G., "Modal Propagation Angles in a Cylindrical Duct and Their Relation to Sound Radiation," Technomic Publishing Company, Inc., Lancaster, PA, NASA TM-79030 Jan. 1979; also AIAA Paper 79-0183, Jan. 1979.

⁹Sutliff, D. L., and Nagel, R. T., "Development of an Active Noise Control System for Ducted Fans (Without Acoustic Feedback)," *Proceedings of the Second Conference on Recent Advances in Active Control of Sound and Vibration*, Technomic Publishing Company, Inc., Lancaster, PA, 1993, pp. 825-836.

¹⁰Ikelheimer, B. J., "Active Noise Control of Acoustic Modes from a Ducted Fan," M.S. Thesis, North Carolina State Univ., Dept. of Mechanical and Aerospace Engineering, Raleigh, NC, Dec. 1994.

AEROSPACE FACTS AND FIGURES, 1993-1994

AEROSPACE FACTS AND FIGURES, 1993-1994

AEROSPACE FACTS AND FIGURES, 1993-1994

AEROSPACE FACTS AND FIGURES, 1993-1994

AEROSPACE FACTS AND FIGURES, 1993-1994

This book, published by Aerospace Industries Association, is the most complete one-stop data source on the U.S. aerospace industry that you'll find. It features more than 140 statistical tables showing trends over time in the U.S. aerospace industry. Tables are updated through 1992. Selected tables include 1993 and 1994 estimates based on U.S. government budget projections.

You'll find updates on aerospace sales; shipments, orders, and backlog of aircraft, engines, and parts;

production of U.S. civil and military aircraft; outlays for missile procurement by military service; space activities outlays by federal agency; world and U.S. aircraft fleet data; aerospace R&D funding; U.S. aerospace trade; U.S. aerospace employment by sector; aerospace profits, capital investment, and industry balance sheets.



**Aerospace
Industries
Association**

**1993, 176 pp, Paperback
\$25.00 each
Order #: AFF-94(945)**

Place your order today! Call 1-800/682-AIAA



American Institute of Aeronautics and Astronautics

Publications Customer Service, 9 Jay Gould Ct., P.O. Box 753, Waldorf, MD 20604
FAX 301/843-0159 Phone 1-800/682-2422 8 a.m. - 5 p.m. Eastern

Sales Tax: CA residents, 8.25%; DC, 6%. For shipping and handling add \$4.75 for 1-4 books (call for rates for higher quantities). Orders under \$100.00 must be prepaid. Foreign orders must be prepaid and include a \$20.00 postal surcharge. Please allow 4 weeks for delivery. Prices are subject to change without notice. Returns will be accepted within 30 days. Non-U.S. residents are responsible for payment of any taxes required by their government.